An Improved Predictive Control Approach for Output Feedback in Hybrid Systems

Zahra Rabiee Fard, Mustafa Rostami, Soroush Sadeghnejad*

Biomedical Engineering Department, Amirkabir University of Technology (Tehran Polytechnic)

*Corresponding Author Email: s.sadeghnejad@aut.ac.ir

ACCEPTED MANUSCRIPT

Abstract: An enhanced robust output-feedback quasi-min–max model predictive control (MPC) scheme is proposed for linear parameter-varying (LPV) and hybrid systems. Building on the quasi-min–max framework, the cost function is reformulated in terms of the input increment Δu rather than the absolute control effort. One-step predictive dynamics consistent with this formulation are incorporated to mitigate switching-induced disturbances in the control signal. Combined with the natural convention $u(-1)=0$, the proposed approach enforces a zero initial control action by construction. These practical modifications result in smoother control signals while maintaining robust stability under input constraints. An offline robust state observer is designed via linear matrix inequalities to estimate the unmeasurable system states from output feedback. The effectiveness of the method is demonstrated on a hybrid LPV system under both predefined and random switching signals. Simulation results show that the control input remains within the prescribed amplitude bounds, starts from zero, and exhibits noticeably reduced fluctuations at switching instants compared with the conventional quasi-min–max approach. Although a slight increase in the output root-mean-square error is observed, the significant improvement in control smoothness confirms the practical advantage of the Δu-based formulation for hybrid and LPV systems subject to input constraints.

Keywords: Model predictive control, Linear parameter-varying systems, Hybrid systems, Robustness, Quasi-min-max algorithm.

1. INTRODUCTION

It is well known that linear dynamic models cannot generally capture the nonlinear characteristics present in most physical systems [1-4]. Although various nonlinear control methods exist for such

systems, they are often computationally demanding to implement [5–7]. Piecewise linear approximation is a widely used alternative that reduces this computational burden while preserving a tractable control-design procedure [8-10]. However, the switching phenomenon inherent to piecewise linear dynamics can render the control signal discontinuous, causing abrupt changes in system behavior. Controlling such systems becomes further complicated when constraints on control input, output, and state variables must be respected simultaneously with robustness against model uncertainty [9].

Model Predictive Control (MPC), originally introduced as Dynamic Matrix Control (DMC) in the late 1970s [11,12], has since become one of the most widely adopted approaches for constrained multivariable control, with applications spanning refining, petrochemicals, aerospace, mining/metallurgy, and robotics [13–15]. Its popularity stems largely from its native ability to handle constrained, switching, multiple-input multiple-output (MIMO) systems [16–18]. However, like other model-based techniques, MPC requires an accurate dynamic model and reliable state estimation, motivating sustained research into robust formulations that guarantee stability under model uncertainty [19–21].

Robustness in MPC has been pursued along several lines. Minimax formulations were studied by Pavlov et al. [4], while linear matrix inequality (LMI)-based robust constrained MPC was proposed to handle model uncertainty explicitly [22]. Lu and Arkun [23] introduced a quasi-min–max algorithm for linear parameter-varying (LPV) and linear time-invariant (LTI) systems under the assumption of full state measurability — an assumption subsequent studies [24, 25] have largely retained. Because exact state measurability is often unrealistic in practice, a smaller body of work has pursued output-feedback MPC instead [26]. Wan and Kothare [27] extended their earlier method [28] into an off-line, robust output-feedback MPC for constrained LTV systems, and Park et al. [29] later proposed an on-line robust output-feedback MPC for LPV systems based on the quasi-min–max algorithm, guaranteeing robust stability under input constraints. However, the method in [29] does not ensure smooth control behavior across transitions between piecewise linear regions, and its control law does not enforce a zero initial control action — both of which are practically significant limitations when continuous, implementation-ready control signals are required.

It is worth clarifying the relationship between LPV and hybrid systems in the present context. LPV systems are characterized by parameters that vary continuously, or within a bounded set, such that the dynamics can be expressed as a convex combination of local linear models [30]. Hybrid (switched) systems, in contrast, involve discrete transitions among a finite number of subsystems [31]. Many practical applications — particularly in biomedical robotics — exhibit both features

ACCEPTED MANUSCRIPT

simultaneously. Hybrid LPV systems are therefore considered, in which a switching signal selects the active operating mode (for example, different tissue interaction regimes) while, within each mode, the system evolves as an LPV model with measurable scheduling parameters. This combined framework enables the controller to handle both abrupt mode switches and continuous parameter variation. In this paper, we consider hybrid LPV systems, where a switching signal selects the active operating mode (e.g., different tissue interaction regimes) while, within each mode, the system evolves as an LPV model with measurable scheduling parameters. This combined framework allows the controller to handle both abrupt mode switches and continuous parameter variation.

Beyond the work of Park et al. [29], recent output-feedback MPC research for LPV and hybrid systems has progressed along three broadly complementary directions. From a model-based robustness standpoint, tube-based and constraint-tightening formulations have been proposed to reduce the conservatism of worst-case min–max optimization while still relying on an explicit polytopic model of the parameter-dependent dynamics [32, 33]; related work has also examined multi-step output-feedback robust MPC that exploits bounded rates of parameter change to tighten estimation-error and uncertainty sets over the prediction horizon [34]. In parallel, a growing body of work seeks to relax the dependence on an explicit scheduling model altogether: data-driven predictive control has been formulated directly from input–output trajectory data for LPV systems [35], and data-driven min–max MPC has been proposed specifically for LPV systems with an unknown scheduling signal [36]. For switched dynamics, robust MPC designs based on Lyapunov–Metzler stability conditions have been developed to handle mode transitions with formal stability guarantees [37], and, most recently, learning-augmented MPC schemes have begun to appear for switched nonlinear systems, where an online-learned model adapts the predictive dynamics across operating modes [38].

Despite this progress, none of the above directions simultaneously addresses three practical requirements: (i) smooth control effort across switching instants, (ii) an output-feedback structure that does not assume full state measurability, and (iii) a guaranteed zero initial control action. In particular, the data-driven and learning-based approaches in [35–38] still inherit the absolute-control-effort cost structure of [23] and [29], and therefore remain susceptible to the same switching-induced discontinuities that motivate the present work. This gap is addressed by enhancing the quasi-min–max output-feedback MPC framework of Park et al.[29] through a redefined, increment-based cost function combined with one-step predictive dynamics.

ACCEPTED MANUSCRIPT

An improved quasi-min–max output-feedback MPC approach tailored for LPV and hybrid systems is proposed. Building on [29], the same measurability assumption for current system parameters is adopted, but the formulation departs from the earlier work in two respects. First, the optimization cost function is reformulated in terms of the input increment Δu rather than the absolute control effort u—in contrast to [29] , which penalizes u directly—and one-step predictive dynamics consistent with this formulation are incorporated, thereby mitigating switching-induced disturbances in the control law. Second, combined with the natural convention $u(-1) := 0$, this reformulation ensures that the initial control signal is zero by construction, rather than by post-hoc observation.

The main contributions of the present work are as follows:

The present paper addresses this gap by enhancing the quasi-min–max output-feedback MPC framework of Park et al. [29] through a redefined, increment-based cost function combined with one-step predictive dynamics.

In this paper, we propose an improved quasi-min–max output-feedback MPC approach tailored for LPV and hybrid systems. Building on [29], we adopt the same measurability assumption for current system parameters, but depart from it in two respects. First, we reformulate the optimization cost function in terms of the input increment Δu rather than the absolute control effort u — in contrast to [29], which penalizes u directly — and incorporate one-step predictive dynamics consistent with this formulation, which mitigates switching-induced disturbances in the control law. Second, combined with the natural convention $u(-1) := 0$, this reformulation ensures that the initial control signal is zero by construction, rather than by post hoc observation.

Our proposed framework presents the following key contributions:

1. A redefined cost function based on the input increment Δu, incorporating one-step predictive dynamics consistent with this formulation, which eliminates switching-induced disturbances while enforcing zero initial control action by construction.
2. A comparative analysis (Section 2.3.1) that explicitly contrasts the proposed formulation against [23] and [29] along these dimensions, together with a numerical demonstration on a hybrid LPV system under both predefined and random switching signals.

2. PROBLEM STATEMENT

ACCEPTED MANUSCRIPT

2.1. Description of the Dynamic System

Consider a MIMO linear parameter variable (LPV) discrete-time system, described by the following dynamic model:

$$\begin{aligned}\mathbf{x}(k+1) &= \mathbf{A}(s(k))\mathbf{x}(k)+\mathbf{B}(\mathbf{s}(k))\mathbf{u}(k)\\ \mathbf{y}(k) &= \mathbf{C}(s(k))\mathbf{x}(k)\end{aligned} \tag{1}$$

in which, $\mathbf{x}(k)\in\mathbf{R}^{\mathbf{n_x}}$ is the unmeasurable state of the system, $\mathbf{y}(k)\in\mathbf{R}^{\mathbf{n_y}}$ is the measurable output, $\mathbf{u}(k)\in\mathbf{R}^{\mathbf{n_u}}$ is the control input, and $s(k)$ is the time-varying switching signal, which is measurable at each step k and can be defined either dependent on or independent of the dynamic system. It is assumed that $\left[\mathbf{A}(s(k)),\mathbf{B}(s(k)),\mathbf{C}(s(k))\right]\in\boldsymbol{\Omega}\equiv\mathbf{C}_0\left\{\left[\mathbf{A_i},\mathbf{B_i},\mathbf{C_i}\right]\right\}$ varies inside a corresponding polytope $\boldsymbol{\Omega}$ whose vertices consist of $\mathbf{L_g}$ local system matrices (number of piece-wise linear regions) and are known at each step k. Besides, $\mathbf{C}_0$ denotes the convex hull of the aforementioned polytope.

2.2 Design of Off-Line Robust Observer

In the previous section, the dynamics of an LPV discrete-time system were introduced. Given that the states of the system are unmeasurable, an off-line, robust observer is used based on [29]. In this study, as the states of system (1) are unmeasurable, we use the following state observer to estimate the system's unknown states:

$$\hat{\mathbf{x}}(k+1)=\mathbf{A}(s(k))\hat{\mathbf{x}}(k)+\mathbf{B}(s(k))\mathbf{u}(k)+\mathbf{L}_0\left(\mathbf{y}(k)-\mathbf{C}(s(k))\hat{\mathbf{x}}(k)\right) \tag{2}$$

where, $\hat{\mathbf{x}}(k)$ is the estimated state of the system and $\mathbf{L}_0$ is the observer gain, which is necessary to be determined in terms of LMIs. Note that, since we know the current system matrices $\left[\mathbf{A}(s(k))\right]$ and $\left[\mathbf{B}(s(k))\right]$, the output $\mathbf{y}(k)$, and the estimated $\hat{\mathbf{x}}(k)$ at each step *k*, $\hat{\mathbf{x}}(k+1)$ can be calculated using the state observer (2), whereas $\hat{\mathbf{x}}(k+1+i)$, $i\geq 1$, is uncertain.

Park et al.[29] designed an off-line robust observer in order to estimate the states of the dynamic system from its output feedback. In this regard, the estimation error of states is defined as $\mathbf{e}(k)=\mathbf{x}(k)-\hat{\mathbf{x}}(k)$. Considering Eqs. (1) and (2), the error dynamics can be defined as:

ACCEPTED MANUSCRIPT

$$\mathbf{e}(k+1)=\left(\mathbf{A}(s(k))-\mathbf{L}_0\mathbf{C}(s(k))\right)\mathbf{e}(k) \tag{3}$$

where $[\mathbf{A}(s(k))|\mathbf{B}(s(k))] \in \boldsymbol{\Omega}$. In the following, we determine the observer gain $\mathbf{L}_0$ in terms of LMI. Consider a quadratic function for the estimation error $\mathbf{e}(\mathbf{k})$, as $\mathbf{E}(\mathbf{e}(k))$,

$$\mathbf{E}(\mathbf{e}(k))=\mathbf{e}(k)^{\mathrm{T}}\mathbf{P}_0\mathbf{e}(k),\mathbf{P}_0>0 \tag{4}$$

in which, $\mathbf{P}_0$ is a positive definite matrix. If $\mathbf{E}(\mathbf{e}(k))$ satisfies the stability condition:

$$\mathbf{E}(\mathbf{e}(k+1+i))-\rho^2\mathbf{E}(\mathbf{e}(k+i))<-\mathbf{e}(k+i)^{\mathrm{T}}\mathbf{L}_{\mathbf{e}}\mathbf{e}(k+i) \tag{5}$$

If condition (5) is satisfied, the estimation error dynamics are exponentially stable, which guarantees that the estimation error converges to zero, i.e, $\mathbf{e}(k)\to 0$ as $k\to\infty$. In Eq. (5), for $\mathrm{i}\geq 0$, ρ and $\mathbf{L}_{\mathbf{e}}$ are the decay rate and the weighting matrix respectively and are determined by the designer. Substituting $\boldsymbol{\Lambda}(k+i)=\mathbf{A}(\mathbf{s}(k+i))-\mathbf{L}_0\mathrm{C}(\mathrm{s}(\mathrm{k}+\mathrm{i}))$ in Eq. (5), the equation can be rewritten as follow:

$$\rho^2\mathbf{P}_0-\mathbf{L}_{\mathbf{e}}-\boldsymbol{\Lambda}(k+i)^{\mathrm{T}}\mathbf{P}_0\boldsymbol{\Lambda}(k+i)>0 \tag{6}$$

Using the Schur complement [31], Eq. (6) is explained as:

$$\rho^2\mathbf{P}_0-\mathbf{L}_{\mathbf{e}}-\left(\mathbf{P}_0\boldsymbol{\Lambda}(k+i)\right)^{\mathrm{T}}\mathbf{P}_0^{-1}\left(\mathbf{P}_0\boldsymbol{\Lambda}(k+i)\right)>0 \tag{7}$$

By using the Schur complement [31]it is possible to cast the inequality (7) in the following form:

$$\begin{bmatrix}\rho^2\mathbf{P}_0-\mathbf{L}_{\mathbf{e}} & *\\ \mathbf{P}_0\boldsymbol{\Lambda}(k+i) & \mathbf{P}_0\end{bmatrix}>0. \tag{8}$$

Substituting $\mathbf{Y}_0:=\mathbf{P}_0\mathbf{L}_0$ we see that (8) is equivalent to:

$$\begin{bmatrix}\rho^2\mathbf{P}_0-\mathbf{L}_{\mathbf{e}} & *\\ \mathbf{P}_0\mathbf{A}(p(k+i))-\mathbf{Y}_0\mathbf{C} & \mathbf{P}_0\end{bmatrix}>0. \tag{9}$$

ACCEPTED MANUSCRIPT

Since the inequality (9) is affine in $\left[\mathbf{A}\left(p(k+i)\right)\ \mathbf{B}\left(p(k+i)\right)\right]$, it is satisfied for all $\left[\mathbf{A}\left(p(k+i)\right)\ \mathbf{B}\left(p(k+i)\right)\right] \in \mathbf{\Omega}$ and since $\mathbf{\Omega}$ is a convex polytope with vertices $\left[\mathbf{A}_j, \mathbf{B}_j, C_j\right]$, $j = 1, .\, .L$, satisfaction over the entire polytope is guaranteed If and only if there exist $\mathbf{P}_0 > 0$ and $\mathbf{Y}_0$ such that

$$\begin{bmatrix} \rho^2 \mathbf{P}_0 - \mathbf{L}_e & * \\ \mathbf{P}_0 \mathbf{A}_j - \mathbf{Y}_0 \mathbf{C} & \mathbf{P}_0 \end{bmatrix} > 0,\ j = 1, 2, \ldots, L. \tag{10}$$

In Eq. (8), (9) and (10) * denotes the transpose of $\mathbf{P}_0\mathbf{A}_j - \mathbf{Y}_0\mathbf{C}$ .the observer gain $\mathbf{L}_0$ is given by $\mathbf{L}_0 = \mathbf{P}_0^{-1}\mathbf{Y}_0$ and hence the estimated state vector $\hat{\mathbf{x}}(k)$ in Eq. (2) converges to the real states of the system $\mathbf{x}(k)$.

In summary, if there exists a $\mathbf{P}_0 > 0$ and $\mathbf{Y}_0 = \mathbf{P}_0\mathbf{L}_0$ which satisfies the constraint of Eq. (8), then the obtained observer gain $\mathbf{L}_0$ and the stability of the dynamic error of Eq. (4) can be guaranteed for any $\left[\left(\mathbf{A}(s(k))|\mathbf{B}(s(k))\right)\right] \in \mathbf{\Omega}$ and finally, as $k \to \infty$, one can conclude that $\hat{\mathbf{x}}(k) \to \mathbf{x}(k)$.

2.3. MPC-Based Control with On-Line Output Feedback

To achieve the desired control function for a dynamic system, such as the regulation of the output signal, it is essential to first define the cost function and the constraints of the system. Subsequently, based on the assumptions and concepts presented in Section 2.2, the objective is to design a control scheme that can stabilize the system by optimizing the cost function while satisfying the associated constraints.

The following assumptions are made throughout this section:

A1. The current system matrices $\mathbf{A}(s(k)), \mathbf{B}(s(k))$, and $\mathbf{C}(s(k))$ are known at each sampling instant k , since the switching signal s(k) is measurable.

A2. The future system matrices for $k+i$ ($i \geq 1$) belong to a known polytope (Ω).

ACCEPTED MANUSCRIPT

A3. The pair $\left(\mathbf{A}\left(s(k)\right),\mathbf{B}\left(s(k)\right)\right)$ is stabilizable and $\left(\mathbf{A}\left(s(k)\right),\ \mathbf{C}\left(s(k)\right)\right)$ is detectable for all admissible *s(k)*.

A4. The control input satisfies the amplitude constraints

$$\left|\mathbf{u}_{\mathbf{j}}(\mathbf{k})\right| < \mathbf{u}_{\mathbf{j,max}} \qquad \mathrm{j}=1,2,\ldots,\mathrm{n_u} \qquad \mathrm{k}\geq 0 \qquad (11)$$

A5. The robust observer designed in Section 2.2 ensures that the estimation error $\mathbf{e}(k)=\mathbf{x}(k)-\hat{\mathbf{x}}(k)$ as $k\to\infty$

Remark (Practical justification and limitations of A1). Measurability of *s(k)* holds when the switching signal is determined by a directly sensed physical quantity, such as a measurable position or force threshold. Small measurement noise in *s(k)* is implicitly tolerated by the polytopic uncertainty set **Ω**, whereas persistent misclassification of the active mode invalidates the robust stability guarantee, since **Ω** presumes correct vertex identification. Alternative approaches, such as dwell-time-based switching detection or recursive parameter estimation, may be used to obtain a reliable estimate of *s(k)* in such cases.

Since in the works of Lu and Arkun [23] and Park et al.[29], future states are not explicitly predicted, the predictive capability of the dynamic model is not fully exploited. However, because the current state of the system is either measured or accurately estimated by the observer, the predictive model can forecast the system behavior one or more steps ahead. This reduces the uncertainty in future predictions and leads to less conservative control actions.

Accordingly, the central contribution of this study is the reformulation of the cost function using input increments *Δu* instead of the absolute control effort u, incorporating one-step predictive dynamics consistent with this formulation. This modification effectively mitigates unwanted disturbances caused by abrupt switching and discontinuities in the control signal. Furthermore, adopting the convention that no control action exists prior to the initial time instant, it enforces a zero initial control action by construction, which is highly desirable from a practical implementation standpoint. Overall, these enhancements ensure constraint satisfaction and robust stability while producing smoother control signals across switching instants.
In our model predictive control scheme, the following predictive model is introduced to forecast the future states of the system (1):

$$\hat{\mathbf{x}}_{\mathbf{p}}(k+1+i|k)=\mathbf{A}\left(s(k+i)\right)\hat{\mathbf{x}}_{\mathbf{p}}(k+i|k)+\mathbf{B}\left(s(k+i)\right)\mathbf{u}(k+i|k)$$
$$\hat{\mathbf{x}}_{\mathbf{p}}(k|k)=\hat{\mathbf{x}}(k), \qquad \mathrm{i}\geq 1 \qquad (12)$$

Where $\hat{\mathbf{x}}_{\mathbf{p}}(k+i|k)$ denotes the predicted state of $\mathbf{x}(k+i)$ of the system in Eq. (1), and $\mathbf{u}(k)$ is the future control input for step $k+i$ considered at step k. For this purpose, assume that

ACCEPTED MANUSCRIPT

$\hat{\mathbf{x}}_{\mathbf{p}}(k|k) := \hat{\mathbf{x}}(k)$, and the first element of the computed control sequence is $\mathbf{u}(k) = \mathbf{u}(k \mid k)$. In the future steps, $\mathbf{u}(k+i|k)$ is estimated as follows:

$$\mathbf{u}(k+i|k) = \boldsymbol{\Psi}(k)\hat{\mathbf{x}}_{\mathbf{p}}(k+i|k), \qquad \mathrm{i} \geq 1 \tag{13}$$

where, $\boldsymbol{\Psi}(k)$ is the future feedback gain introduced at step k. Using the optimization strategy introduced in [29] , this method proposes to minimize the infinite horizon objective function $\mathrm{J}_0^{\infty}(\mathrm{k})$ at each step k as:

$$\begin{gathered} \min_{\mathbf{u}(k+i|k)} \max_{\left[\left(\mathbf{A}(s(k+i))|\mathbf{B}(s(k+i))\right)\right] \in \Omega, i \geq 0} J_0^{\infty}(k) \\ J_0^{\infty}(k) = J_0^1(k) + J_1^{\infty}(k) \end{gathered} \tag{14}$$

From a physical and control-engineering standpoint, penalizing the absolute control effort $\mathbf{u}(k)$, as in [23] and [29], does not distinguish between a large but steady actuation and an abrupt jump caused by switching between piecewise linear regions. In robotic systems, such abrupt jumps translate directly into mechanical jerk and increased actuator wear, even when $\mathbf{u}(k)$ remains within its admissible bound. Penalizing the input increment $\Delta\mathbf{u}(k) = \mathbf{u}(k) - \mathbf{u}(k-1)$ instead directly targets this rate of change — the quantity most closely associated with actuator stress — rather than the control magnitude itself. This motivates the reformulation of the cost function in Eqs. (14)–(15).

The input constraints from (11) should be added to Eq. (14). The terms in (14) are expressed as follows:

$$\begin{cases} \triangle\mathbf{u}(k) = \mathbf{u}(k) \\ \triangle\mathbf{u}(k) = \mathbf{u}(k) - \mathbf{u}(k-1) \qquad k > 1 \end{cases}$$

$$J_0^{\infty}(k) = \sum_{\mathrm{i}=0}^{\infty} \left\{ \hat{\mathbf{x}}_{\mathbf{p}}(k+i|k)^{\mathrm{T}} \mathbf{Q}\, \mathbf{x}_{\mathbf{p}}(k+i|k) + \triangle u(k+i|k)^{\mathrm{T}} \mathbf{R}\, \triangle u(k+i|k) \right\}$$

$$J_0^1(k) := \hat{\mathbf{x}}_{\mathbf{p}}(\mathrm{k}|\mathrm{k})^{\mathrm{T}} \mathbf{Q} \hat{\mathbf{x}}_{\mathbf{p}}(k|k) + \triangle u(k|k)^{\mathrm{T}} \mathbf{R}\, \triangle u(k|k)$$

$$J_1^{\infty}(k) = \sum_{\mathrm{i}=1}^{\infty} \left\{ \hat{\mathbf{x}}_{\mathbf{p}}(k+i|k)^{\mathrm{T}} \mathbf{Q} \hat{\mathbf{x}}_{\mathbf{p}}(k+i|k) + \triangle u(k+i|k)^{\mathrm{T}} \mathbf{R}\, \triangle u(k+i|k) \right\} \tag{15}$$

$$J_1^{\infty}(k) := \sum_{\mathrm{i}=1}^{\infty} \left\{ \hat{\mathbf{x}}_{\mathbf{p}}(k+i|k)^{\mathrm{T}} \mathbf{Q} \hat{\mathbf{x}}_{\mathbf{p}}(k+i|k) + \triangle u(k+i|k)^{\mathrm{T}} \mathbf{R} \triangle u(k+i|k) \right\} = \hat{\mathbf{x}}_{\mathbf{p}}(k+1|k)^{\mathrm{T}} \mathbf{Q} \hat{\mathbf{x}}_{\mathbf{p}}(k+1|k) + J_2^{\infty}$$

ACCEPTED MANUSCRIPT

$$J_2^{\infty} = \sum_{i=2}^{\infty} \left\{ \hat{\mathbf{x}}_{\mathbf{p}} \left(k+i|k \right)^{\mathrm{T}} \mathbf{Q} \hat{\mathbf{x}}_{\mathbf{p}} \left(k+i|k \right) \right\} + \sum_{i=1}^{\infty} \left\{ \triangle u \left(k+i|k \right)^{\mathrm{T}} \mathbf{R} \triangle u \left(k+i|k \right) \right\}$$

Remark (Zero initial control by construction). Since no control action is applied prior to the initial time instant, we adopt the convention $u(-1) := 0$. Under Eq. (15), this gives $\Delta u(1) = \boldsymbol{u}(1)$, so that the term $\mathbf{B}(s(1))\mathbf{u}(0)$ vanishes from the predictive dynamics (12) at the first step. Because the cost function $J_1^0(k)$ in (15) penalizes $\Delta u(k)$ rather than $\mathbf{u}(k)$ directly, the optimization (46) drives the first control action toward zero from the structure of the problem itself — unlike [29], where **u**(0|0) is penalized as an absolute effort with no mechanism enforcing a zero initial value.

Where **R>0** and **Q> 0** are the weight matrices. By introducing an upper bound on J_2^{∞}, differing from the approach proposed in [23, 29], the quasi-min–max optimization problem for MPC can be derived. This is achieved by defining the following Switched Quadratic Lyapunov function:

The stability analysis in this subsection follows the standard Lyapunov-based argument for quasi-min–max MPC established in [23] and [29], restated here using the notation $\mathbf{\Gamma}(k)$ and $\hat{\mathbf{x}}_{\mathbf{p}}(k+i\,|\,k)$ consistent with the predictive dynamics introduced above. The specific theoretical contribution of this work does not lie in this generic Lyapunov argument itself, but in how the resulting performance bound is subsequently combined with the redefined **Δu**-based cost structure, as detailed later in this section and analyzed comparatively in Section 2.3.1.

$$V\left(\hat{\mathbf{x}}_{\mathbf{p}} \left(k+i|k \right) \right) = \hat{\mathbf{x}}_{\mathbf{p}} \left(k+i|k \right)^{\mathrm{T}} \mathbf{\Gamma}(k) \hat{\mathbf{x}}_{\mathbf{p}} \left(k+i|k \right), \quad i>0,\ \mathbf{\Gamma}(k) > 0 \tag{16}$$

it is assumed that $V\left(\hat{\mathbf{x}}_{\mathbf{p}} \left(k+i|k \right) \right)$ satisfies the following stability condition at each step *k* for $\left[\left(\mathbf{A}\left(s\left(k+i \right) \right) | \mathbf{B}\left(s\left(k+i \right) \right) \right) \right] \in \Omega, \mathrm{i} \geq 1$. Consequently, Eq. (16) can be reformulated as follows:

$$V_{\mathrm{k+i}} = \mathbf{Xp}_{\mathbf{k+i}} \mathbf{\Gamma}_{\mathbf{k}} \mathbf{Xp}_{\mathbf{k+i}} \tag{17}$$

Eq. (17) is valid for any subsequent action that leads to the following relation:

$$\begin{aligned} V_{k+i+1} - V_{k+i} &< -J_{k+i}^{k+i+1} \\ J_{k+i}^{k+i+1} &= \mathbf{Xp}_{\mathbf{k+i}} \mathbf{Q} \mathbf{Xp}_{\mathbf{k+i}} + \triangle \mathbf{u}_{\mathbf{k+i}}^{\mathbf{T}} \mathbf{R} \triangle u_{k+i} \end{aligned} \tag{18}$$

To guarantee the stability of the system, it is necessary that $\mathrm{V}\left(\hat{\mathrm{x}}_{\mathrm{p}} \left(\infty | \mathrm{k} \right) \right) = 0$. Additionally, it is essential to optimize all cost functions for all future steps. Consequently, the stability criterion in Eq.

ACCEPTED MANUSCRIPT

(18) for each future step is incorporated into the criteria of other steps to establish an upper bound for the summation of all cost functions based on V_k and V_{k+1}. In this work, the control law is derived based on *V(k)*. This choice offers several advantages compared to the derivation from *V(k+1)* used in previous studies such as Park et al. [29], which will be discussed later. Accordingly, the control law in the proposed approach is considered as follows:

$$J_0^{\infty}(k) < V_k \tag{19}$$

where

$$J_2^{\infty} + \mathbf{X}p_{k+1}^{T}\boldsymbol{QXp}_{\boldsymbol{k}+1} + J_0^1 < V_k \tag{20}$$

or

$$J_2^{\infty} < V_k - \mathbf{Xp}_{\mathbf{k}+1}^{\mathbf{T}}\mathbf{QXp}_{\mathbf{k}+1} - J_0^1 \tag{21}$$

In Eq. (21), the left side of the inequality is indefinite, while the right side represents the maximum of J_2^{∞}. By optimizing the cost function while satisfying the input constraints, the control input is defined as follows:

$$maxJ_2^{\infty} < \delta(k) \tag{22}$$

where, $\boldsymbol{\delta}(k)$ is a non-negative variable to be minimized. Considering (22) for each time step, the following relation can be derived:

$$V_k - \mathbf{Xp}_{\mathbf{k}+1}^{\mathbf{T}}\mathbf{QXp}_{\mathbf{k}+1} - J_0^1 < \delta(k) \tag{23}$$

To ensure the positive definiteness of the Lyapunov matrix and to prevent the invariant ellipsoid from becoming excessively large (which could weaken the stability guarantee), the following additional constraint is imposed [29]:

$$\boldsymbol{\Gamma}(k) > \varepsilon \mathrm{I} \quad \text{for} \quad \varepsilon > 0$$

where ε is a small positive scalar. This condition guarantees a minimum eigenvalue for $\boldsymbol{\Gamma}(k)$, thereby ensuring the robustness of the closed-loop stability and the well-posedness of the optimization problem.

In summary, to guarantee the stability of an LPV system with input constraints using MPC, the quasi-min–max optimization problem of Eq. (12) must be solved in order to find the $\mathbf{u}(k|k)$ as the control input and $\boldsymbol{\Psi}(k)$ as the future feedback gain. Henceforth, we focus on the design of the MPC scheme for an LPV system with LMI constrints and solve the quasi-min-max optimization

ACCEPTED MANUSCRIPT

problem of the infinite horizon MPC scheme. This approach involves finding the solutions for $\mathbf{u}(k) := \mathbf{u}(k|k)$ and $\mathbf{\Psi}(\mathrm{k})$ by solving the optimization problem in Eq. (14) while guaranteeing the stability of the system and considering the effects of constraints on the performance and input variables. Thus, the following functions can be defined:

$$V_k = \mathbf{Xp_k^T \Gamma_k Xp_k}$$

$$\mathbf{Xp_{k+1}} = \mathbf{A_k Xp_k} + \mathbf{B_k} \triangle \mathbf{u}(k) + \mathbf{L_o}\left(\mathbf{y}(\mathrm{k}) - \mathbf{C_k}\hat{\mathrm{X}}_{\mathrm{k}}\right) + \mathbf{B_k u}(k-1) \tag{24}$$

$$\mathrm{J}_0^1 = \mathbf{Xp_k^T Q Xp_k} + \triangle \mathbf{u_k^T R} \triangle \mathbf{u_k}$$

Considering Eqs. (23) and (24), Eq. (23) can be rewritten as:

$$\mathbf{Xp_k^T \Gamma_k Xp_k} - \left(\mathbf{Xp_k^T} + \mathbf{Xp_k^T A_k^T}\right)\mathbf{Q}\left(\mathbf{Xp_k} + \mathbf{A_k Xp_k}\right) - \triangle u^T\left(\mathbf{B^T QB}\right)\triangle u - \triangle u^T \mathbf{R} \triangle u - \left[\mathbf{L_o}\left(\mathbf{y} - \mathbf{C_k}\hat{\mathbf{X}}_{\mathbf{k}}\right) + \mathbf{B_k u}(k-1)\right]^{\mathrm{T}} \mathbf{Q}\left[\mathbf{L_o}\left(\mathbf{y} - \mathbf{C_k}\hat{\mathbf{X}}_{\mathbf{k}}\right) + \mathbf{B_k u}(k-1)\right] < \delta_{\mathrm{k}} \tag{25}$$

Assuming that $\mathbf{\Gamma_k} = \delta \mathbf{\Phi}^{-1}{}_{\mathrm{k}}$ in (25), the following expression can be derived:

$$\delta\tau_{\mathrm{k}} = \left(\mathbf{Xp_k^T} + \mathbf{Xp_k^T A_k^T}\right)\mathbf{Q}\left(\mathbf{Xp_k} + \mathbf{A_k Xp_k}\right) + \triangle u^T\left(\mathbf{B^T QB} + \mathbf{R}\right)\triangle u + \left[\mathbf{L_o}\left(\mathbf{y} - \mathbf{C_k}\hat{\mathbf{X}}\mathbf{p_k}\right) + \mathbf{B_k u}(k-1)\right]^{\mathrm{T}} \mathbf{Q}\left[\mathbf{L_o}\left(\mathbf{y} - \mathbf{C_k}\hat{\mathbf{X}}_{\mathbf{k}}\right) + \mathbf{B_k u}(k-1)\right] \tag{26}$$

The remainder of this derivation relies on three standard techniques from the robust LMI-based MPC literature: Schur complements, congruence transformations, and a change of variables to eliminate bilinear terms — the same tools underlying the derivations in [23] and [29]. We indicate each step explicitly below rather than treating them as self-evident.

Then, the following inequality can be derived:

$$1 + \tau_k - \mathbf{Xp_k^T \Phi^{-1} Xp_k} > 0 \tag{27}$$

Using the Schur complement, Eq. (27) results in:

$$\begin{bmatrix} 1+\tau_k & * \\ \mathbf{Xp_k} & \mathbf{\Phi}(\mathbf{k}) \end{bmatrix} > 0 \tag{28}$$

Defining the complementary equation and some auxiliary matrices as:

$$\begin{bmatrix} \eta & * \\ \mathbf{Xp_k} & \mathbf{\Phi}(\mathbf{k}) \end{bmatrix} + \mathbf{\Lambda^T \Phi^{-1} \Lambda} > 0$$

$$\Lambda = \begin{bmatrix} \theta^{\frac{1}{2}}\mathbf{Xp_k} & 0 \\ \beta^{\frac{1}{2}} \triangle u_k & 0 \end{bmatrix}, \begin{cases} \theta = \left(\mathbf{I} + \mathbf{A^T}\right)\mathbf{Q}\left(\mathbf{I} + \mathbf{A}\right) \\ \beta = \mathbf{B^T QB} + \mathbf{R} \end{cases}, \tag{29}$$

ACCEPTED MANUSCRIPT

$$\eta = 1 + \left[\mathbf{L_o}\left(\mathbf{y} - \mathbf{C_k}\hat{\mathbf{X}}_\mathbf{k}\right) + \mathbf{B_k}\mathrm{u}\left(k-1\right)\right]^{\mathrm{T}} \mathbf{Q}\left[\mathbf{L_o}\left(\mathbf{y} - \mathbf{C_k}\hat{\mathbf{X}}_\mathbf{k}\right) + \mathbf{B_k}\mathbf{u}\left(k-1\right)\right].$$

Then, by again applying the Schur complement, the aforementioned inequality will result in:

$$\begin{bmatrix} \mathbf{M} & * \\ \mathbf{T} & \mathbf{\Pi} \end{bmatrix} > 0$$

$$\mathbf{M} = \begin{bmatrix} \boldsymbol{\eta} & * \\ \mathbf{Xp_k} & \boldsymbol{\Phi} \end{bmatrix},\ \mathbf{T} = \begin{bmatrix} \theta^{\frac{1}{2}}\mathbf{Xp_k} & 0 \\ \beta^{\frac{1}{2}}\mathbf{u_k} & 0 \end{bmatrix},\ \mathbf{\Pi} = \begin{bmatrix} \delta\mathbf{I} & 0 \\ 0 & \delta\mathbf{I} \end{bmatrix} \tag{30}$$

Hence, for the next step, it is necessary to define a constraint which can guarantee the stability of the system with regard to the future inputs. Substituting $\mathbf{u}\left(k+i|k\right) = \mathbf{\Psi}\left(\mathbf{k}\right)\hat{\mathbf{x}}_\mathbf{p}\left(k+i|k\right)$, $\mathrm{i} \geq 1$, and also considering Eq. (17) and the future states of the prediction model in Eq. (12), we obtain:

$$\hat{\mathbf{x}}_\mathbf{p}\left(k+i|k\right)^{\mathrm{T}} \boldsymbol{\mu}\left(\mathbf{k}\right)\hat{\mathbf{x}}_\mathbf{p}\left(k+i|k\right) - \hat{\mathbf{x}}_\mathbf{p}\left(k+i|k\right)^{\mathrm{T}} \boldsymbol{\omega}\left(k+i\right)^{\mathrm{T}} \mathbf{\Gamma}\left(k\right)\boldsymbol{\omega}\left(k+i\right)\hat{\mathbf{x}}_\mathbf{p}\left(k+i|k\right) > 0 \tag{31}$$

where,

$$\begin{aligned} \boldsymbol{\mu}\left(k\right) &= \mathbf{\Gamma}\left(k\right) - \mathbf{Q} - \mathbf{\Psi}\left(k\right)^{\mathrm{T}}\mathbf{R}\mathbf{\Psi}\left(k\right) \\ \boldsymbol{\omega}\left(k+i\right) &= \mathbf{A}\left(s\left(k+i\right)\right) + \mathbf{B}\left(s\left(k+i\right)\right)\mathbf{\Psi}\left(k\right) \end{aligned} \tag{32}$$

Therefore, the following relation can be derived:

$$\boldsymbol{\mu}\left(k\right) - \boldsymbol{\omega}\left(k+i\right)^{\mathrm{T}} \mathbf{\Gamma}\left(\mathrm{k}\right)\boldsymbol{\omega}\left(k+i\right) > 0 \tag{33}$$

Multiplying by $\delta\left(k\right) > 0$ and pre- and post-multiplying by $\mathbf{\Gamma}\left(k\right)^{-1}$ — a congruence transformation that preserves the sign of the inequality since $\boldsymbol{\delta}\left(k\right)\mathbf{\Gamma}\left(k\right)^{-1}$ is nonsingular — this inequality becomes:

$$\delta(\mathrm{k})\left(\mathbf{\Gamma}(\mathrm{k})^{-1} - \left(\mathbf{\Gamma}(\mathrm{k})^{-1}\right)^{\mathrm{T}}\mathbf{Q}\left(\mathbf{\Gamma}(\mathrm{k})^{-1}\right) - \left(\mathbf{\Psi}(\mathrm{k})\mathbf{\Gamma}(\mathrm{k})^{-1}\right)^{\mathrm{T}} \times \mathrm{R}\left(\mathbf{\Psi}(\mathrm{k})\mathbf{\Gamma}(\mathrm{k})^{-1}\right)\right) - \left(\delta(\mathrm{k})\mathbf{\Gamma}(\mathrm{k})^{-1}\right)^{\mathrm{T}}\ \boldsymbol{\omega}(\mathrm{k}+\mathrm{i})^{\mathrm{T}}\,\delta(\mathrm{k})^{-1} \times \mathbf{\Gamma}(\mathrm{k})\boldsymbol{\omega}(\mathrm{k}+\mathrm{i})\left(\delta(\mathrm{k})\mathbf{\Gamma}(\mathrm{k})^{-1}\right) \tag{34}$$

Considering $\mathbf{\Gamma}\left(k\right) = \delta\left(k\right)\mathbf{\Phi}\left(k\right)^{-1}$ and again using the Schur complement, Eq. (34) can be shown to be equivalent to:

ACCEPTED MANUSCRIPT

$$\begin{bmatrix} \mathbf{N}(k) & * \\ \boldsymbol{\omega}(k+i)\boldsymbol{\Phi}(k) & \boldsymbol{\Phi}(k) \end{bmatrix} > 0 \tag{35}$$

where,

$$\mathbf{N}(k) = \delta(k)\left(\boldsymbol{\Gamma}(k)^{-1} - (\boldsymbol{\Gamma}(k)^{-1}\right)^{\mathbf{T}} \mathbf{Q}\left(\boldsymbol{\Gamma}(k)^{-1}\right) - \left(\boldsymbol{\Psi}(k)\boldsymbol{\Gamma}(k)^{-1}\right)^{\mathbf{T}} \mathbf{R}\left(\boldsymbol{\Psi}(k)\boldsymbol{\Gamma}(k)^{-1}\right) \tag{36}$$

By introducing the change of variables $\mathbf{Y}(k) \coloneqq \boldsymbol{\delta}(k)\boldsymbol{\Phi}(k)$ — a standard substitution used to eliminate the bilinear dependence on $\boldsymbol{\Psi}(\mathbf{k})$ and $\boldsymbol{\Phi}(\mathbf{k})$ and render the inequality affine — Eq. (35) results in:

$$\begin{bmatrix} \boldsymbol{\Phi}(k) & * \\ \mathbf{S}(k) & \boldsymbol{\Phi}(k) \end{bmatrix} - \boldsymbol{\Theta}(k)^{\mathbf{T}} \boldsymbol{\Pi}(k) \boldsymbol{\Theta}(k) > 0 \tag{37}$$

where,

$$\mathbf{S}(\mathbf{k}) = \mathbf{A}\left(s(k+i)\right)\boldsymbol{\Phi}(k) + \mathbf{B}\left(s(k+i)\right)\mathbf{Y}(k)$$

$$\boldsymbol{\Theta}(\mathbf{k}) = \begin{bmatrix} \mathbf{Q}^{\frac{1}{2}}\boldsymbol{\Phi}(k) & 0 \\ \mathbf{R}^{\frac{1}{2}}\mathbf{Y}(K) & 0 \end{bmatrix} \tag{38}$$

Additionally, we can obtain the following matrix inequality using the Schur complement:

$$\begin{bmatrix} \boldsymbol{\Phi}(k) & * & * & * \\ \mathbf{S}(k) & \boldsymbol{\Phi}(k) & * & * \\ \mathbf{Q}^{1/2}\boldsymbol{\Phi}(k) & 0 & \delta(k)\mathbf{I} & * \\ \mathbf{R}^{1/2}\mathbf{Y}(k) & 0 & 0 & \delta(k)\mathbf{I} \end{bmatrix} > 0 \tag{39}$$

where * denotes that the matrix is axisymmetric. The aforementioned inequality, as stated in Eq. (39), is affine in $\left[\left(\mathbf{A}\left(s(k+i)\right)|\mathbf{B}\left(s(k+i)\right)\right)\right]$ if and only if $\mathbf{Y}(k)$ and $\boldsymbol{\Phi}(k)$ exist such that:

ACCEPTED MANUSCRIPT

$$\begin{bmatrix} \mathbf{\Phi}(k) & * & * & * \\ \mathbf{S_j}(k) & \mathbf{\Phi}(k) & * & * \\ \mathbf{Q}^{1/2}\mathbf{\Phi}(k) & 0 & \boldsymbol{\delta}(k)\mathbf{I} & * \\ \mathbf{R}^{1/2}\mathbf{Y}(k) & 0 & 0 & \delta(k)\mathbf{I} \end{bmatrix} > 0, \quad j = 1,2,\ldots,L_g \tag{40}$$

where, $\mathbf{S_j}(k) = \mathbf{A_j}\mathbf{\Phi}(k) + \mathbf{B_j}\mathbf{Y}(k)$ and the general format of the matrix is axisymmetric. Then, it can be denoted that Eq. (23) is satisfied for $\left[\left(\mathbf{A}\left(s(k+i)\right)|\mathbf{B}\left(s(k+i)\right)\right)\right] \in \Omega$. Considering $\mathbf{\Gamma}(k) = \delta(k)\mathbf{\Phi}(k)^{-1}$ for some $\epsilon > 0$, it results in:

$$\delta(\mathrm{k})\mathrm{I} - \epsilon\Phi(\mathrm{k}) > 0 \tag{41}$$

In addition, it is necessary to consider the constraints on the control input, as well as for the future control sequences $\mathbf{u}(k+i|k)$. For these constraints, it is required to define an upper bound for the control input as follows:

$$\left|\mathbf{u}(k+i|k)\right| < \mathbf{u}_{\mathrm{j,\,max}}, \quad j = 1,2,\ldots,n_u, \quad i \geq 1 \tag{42}$$

Hence, it can be concluded that:

$$\max_{\mathrm{i}\geq 1}\left|\mathbf{u}(k+i|k)\right|^2 = \max_{\mathrm{i}\geq 1}\left|\left(\mathbf{Y}\mathbf{\Phi}^{-1}\hat{\mathbf{x}}(k+i|k)\right)_{\mathrm{j}}\right|^2 \leq \max_{\mathrm{i}\geq 1}\left|\left(\mathbf{Y}\mathbf{\Phi}^{-1}\hat{\mathbf{x}}\right)_{\mathrm{j}}\right|^2 \leq \left(\mathbf{Y}\mathbf{\Phi}^{-1/2}\right)_{\mathrm{j2}}^2 = \left(\mathbf{Y}\mathbf{\Phi}^{-1}\mathbf{Y}^{\mathbf{T}}\right)_{\mathrm{jj}} \tag{43}$$

Therefore, if there exists a symmetric matrix, Su, such that:

$$\begin{bmatrix} \mathbf{Su}(k) & * \\ \mathbf{Y}(k)^{\mathbf{T}} & \mathbf{\Phi}(k) \end{bmatrix} > 0 \wedge \mathrm{Su}_{\mathrm{jj}} < \mathrm{u}_{\mathrm{j,\,max}}^2 \quad \mathrm{j} = 1,2,\ldots,\mathrm{n_u} \tag{44}$$

Then, it guarantees that:

$$\left|\mathbf{u}(k+i|k)\right| < \mathbf{u}_{\mathbf{j,max}}, \quad j = 1,2,\ldots,n_u, \quad i \geq 1 \tag{45}$$

Therefore, the input constraint in Eq. (45) is guaranteed for $, j = 1,2,\ldots,n_u, \quad i \geq 1$.

Theorem: Theorem: Suppose Assumptions A1–A5 hold, and suppose the optimization problem in Eq. (46), subject to (12), (13), and (47)–(51), is feasible at some time step k_0 — that is, there exist $\mathbf{u}(k0\,|\,k0)$, $\mathbf{Y}(k0)$, and $\mathbf{\Phi}(k0)$ satisfying (47)–(51) with a finite $\boldsymbol{\delta}(k0)$. Then the optimization

ACCEPTED MANUSCRIPT

problem is feasible at every subsequent step $k > k_0$ (recursive feasibility), and the resulting control law $\mathbf{u}(k+i\,|\,k) = \mathbf{\Psi}(\mathrm{k})\mathbf{x}\hat{}\mathbf{p}(k+i\,|\,k)$, with $\mathbf{\Psi}(k) := \mathbf{Y}(k)\mathbf{\Phi}(k)^{-1}$, guarantees asymptotic robust stability of the closed-loop system, i.e., $\mathbf{x}(k) \to 0$ as $k \to \infty$, for all $[\mathbf{A}(s(k))\,|\,\mathbf{B}(s(k)))] \in \Omega$.

Implementing the aforementioned optimization problem, it can be concluded that:

$$\min_{\mathrm{u(k|k)},\ \mathrm{Y(k)},\ \Phi(\mathrm{k})} \delta(k) \tag{46}$$

$$\begin{bmatrix} \eta & * & * & * \\ \mathbf{Xp_k} & \mathbf{\Phi}(k) & * & * \\ \left((\mathbf{I}+\mathbf{A})^{\mathrm{T}}\mathbf{Q}(\mathbf{I}+\mathbf{A})\right)^{1/2} & \hat{\mathbf{x}}(k) & 0 & \delta(k)\mathbf{I}_{\mathbf{nx*nx}} & * \\ \left(\mathbf{B}^{\mathbf{T}}\mathbf{Q}\mathbf{B}+\mathbf{R}\right)^{1/2} & \blacklozenge \mathrm{u}(k) & 0 & 0 & \delta(k)\mathbf{I}_{\mathbf{nu*nu}} \end{bmatrix} > 0 \tag{47}$$

$$\begin{bmatrix} \mathbf{\Phi}(k) & * & * & * \\ \mathbf{S}_{\mathrm{j}}(k) & \mathbf{\Phi}(k) & * & * \\ \mathbf{Q}^{1/2}\mathbf{\Phi}(k) & 0 & \delta(k)\mathbf{I}_{\mathrm{nx*nx}} & * \\ \mathbf{R}^{1/2}\mathbf{Y}(k) & 0 & 0 & \delta(k)\mathbf{I}_{\mathrm{nu*nu}} \end{bmatrix} > 0, \quad j = 1, 2, \ldots, L_g \tag{48}$$

$$\delta(k)\mathbf{I} - \varepsilon\mathbf{\Phi}(k) > 0 \tag{49}$$

$$\begin{bmatrix} \mathbf{u}_{j,max} & \mathbf{u}_j(k) \\ \mathbf{u}_j(k) & \mathbf{u}_{j,max} \end{bmatrix} > 0 \tag{50}$$

$$\begin{bmatrix} \mathbf{Su}(k) & * \\ \mathbf{Y}(k)^{\mathrm{T}} & \mathbf{\Phi}(k) \end{bmatrix} > 0, \mathbf{Su}_{jj} < \mathbf{u}_{j,max}^2 \quad j = 1, 2, \ldots, \mathrm{n_u} \tag{51}$$

where Eqs. (47) and (48) are axisymmetric matrices and $\eta = 1 + \left[\mathbf{L_o}\left(\mathbf{y} - \mathbf{C_k}\hat{\mathbf{X}}_\mathbf{k}\right)\right]^{\mathrm{T}}\mathbf{Q}\left[\mathbf{L_o}\left(\mathbf{y} - \mathbf{C_k}\hat{\mathbf{X}}_\mathbf{k}\right)\right]$. Additionally,

$$\mathbf{S}_j(k) = \mathbf{A_j}\mathbf{\Phi}(k) + \mathbf{B}_j\mathbf{Y}(k) \tag{52}$$

If $\mathbf{u}(k\,|\,k)$, $\mathbf{Y}(k)$ and $\mathbf{\Phi}(k)$ are available for $\hat{\mathbf{x}}(k)$ and $\mathbf{y}(k)$, the future feedback gain $\mathbf{\Psi}(k)$ results from $\mathbf{\Psi}(k) := \mathbf{Y}(k)\mathbf{\Phi}(k)^{-1}$. Eqs. (47) to (52) are derived from the conditions and

ACCEPTED MANUSCRIPT

inequalities resulting from Eq. (23), the stability criterion in Eq. (18), and $\mathbf{\Gamma}(k) > \varepsilon \mathbf{I}$. If there exist $\mathbf{Y}(k)$, $\mathbf{\Phi}(k)$ and $\delta(\mathrm{k})$ such that Eq. (46) holds and if

$$\hat{\mathbf{x}}_{\mathbf{p}}(k|k)^{\mathrm{T}} \mathbf{Q}\, \hat{\mathbf{x}}_{\mathbf{p}}(k|k) + \triangle \mathrm{u}(k|k)^{\mathrm{T}} \mathbf{R}\, \triangle \mathrm{u}(k|k) + \hat{\mathbf{x}}_{\mathbf{p}}(k+i|k)^{\mathrm{T}} \mathbf{\Gamma}(k) \hat{\mathbf{x}}_{\mathbf{p}}(k+i|k) < \delta(k) \tag{53}$$

Then

$$\hat{\mathbf{x}}_{\mathbf{p}}(k+i|k)^{\mathrm{T}} \mathbf{\Gamma}(k) \hat{\mathbf{x}}_{\mathbf{p}}(k+i|k) < \delta(k) \tag{54}$$

Assuming that $\mathbf{Q}$ and $\mathbf{R}$ are positive definite, and considering Eq. (18), the result can be expressed as:

$$\hat{\mathbf{x}}_{\mathbf{p}}(k+i+1|k)^{T} \mathbf{\Gamma}(k) \hat{\mathbf{x}}_{\mathbf{p}}(k+i+1|k) - \hat{\mathbf{x}}_{\mathbf{p}}(k+i|k)^{\mathrm{T}} \mathbf{\Gamma}(k) \hat{\mathbf{x}}_{\mathbf{p}}(k+i|k) < -\left[\hat{\mathbf{x}}_{\mathbf{p}}(k|k)^{\mathrm{T}} \mathbf{Q}\, \hat{\mathbf{x}}_{\mathbf{p}}(k|k) + \triangle \mathrm{u}(k|k)^{T} \mathbf{R} \triangle \mathrm{u}(k|k)\right], \quad i \geq 1 \tag{55}$$

or equivalently

$$\hat{\mathbf{x}}_{\mathbf{p}}(k+i+1|k)^{\mathrm{T}} \mathbf{\Gamma}(k) \hat{\mathbf{x}}_{\mathbf{p}}(k+i+1|k) < \hat{\mathbf{x}}_{\mathbf{p}}(k+i|k)^{T} \mathbf{\Gamma}(k) \hat{\mathbf{x}}_{\mathbf{p}}(k+i|k), \quad \mathrm{i} \geq 1 \tag{56}$$

Therefore, $\varepsilon := \left\{\hat{\mathbf{x}}_{\mathbf{p}} \in \mathbf{R}^{\mathbf{n}_{\mathrm{x}}} | \hat{\mathbf{x}}_{\mathbf{p}}^{\mathbf{T}} \mathbf{\Gamma}(k) \hat{\mathbf{x}}_{\mathbf{p}} < \delta\right\}$ is an invariant ellipsoid for the predicted future states $\hat{\mathbf{x}}_{\mathbf{p}}(k+i|k), \quad i \geq 1$, of the uncertain system. Then, based on Eqs. (53)-(56), the input constraint can be cast as LMI constraints as presented in Eqs. (42)-(44). To guarantee the robust stability of the system, it is first necessary to ensure that the optimization problem provided in Eq. (46) at step k emains feasible at step $k+1$. This is formulated in the following equation:

$$\begin{aligned} \triangle \mathrm{u}(k+1|k+1) = \triangle \mathrm{u}(k+1|k) &= \mathbf{\Psi}(\mathrm{k}) \hat{\mathbf{x}}_{\mathbf{p}}(k+i|k) \\ \mathbf{\Gamma}(k+1) &= \mathbf{\Gamma}(k) \end{aligned} \tag{57}$$

This shifted sequence satisfies all the LMI constraints (47)–(51) as well as the input constraints, due to the stability condition (27) and the invariant ellipsoid property (56). Therefore, if the optimization problem is feasible at the current time step, it remains feasible at all subsequent time steps. This recursive feasibility property, together with the Lyapunov decrease condition, is fundamental to guaranteeing the asymptotic robust stability of the closed-loop system.

Then, it is necessary to check Eqs. (47), (49), and (50), since they include $s(k)$, $\hat{\mathbf{x}}(k)$, $\mathbf{y}(k)$, and $\mathbf{u}(k|k)$, that change at each step k. First, by the satisfaction of (51) at step k, $\triangle \mathrm{u}(k+1|k)$ is feasible. Then, considering $\triangle \mathrm{u}(k+1|k+1) = \triangle \mathrm{u}(k+1|k) = \mathbf{\Psi}(k) \hat{\mathbf{x}}_{\mathbf{p}}(k+i|k)$, it is clearly stated

ACCEPTED MANUSCRIPT

that (50) is satisfied at step $k+1$. In the next step, (47) should be checked. Based on (47) and Eqs. (54)-(56), the following terms are substituted as $\Delta u(k+1|k+1) = \Delta u(k+1|k) = \boldsymbol{\Psi}(k)\hat{\mathbf{x}}_p(k+i|k)$ and $\boldsymbol{\Gamma}(k+1) = \boldsymbol{\Gamma}(k)$. Then, (47) can be rewritten as

$$\hat{\mathbf{x}}_p(k+1|k)^T \boldsymbol{\zeta}(k) \hat{\mathbf{x}}_p(k+1|k) - \hat{\mathbf{x}}_p(k+1|k)^T \hat{\boldsymbol{\xi}}(k+1)^T \boldsymbol{\Gamma}(k) \hat{\boldsymbol{\xi}}(k+1) \hat{\mathbf{x}}_p(k+1|k) < 0 \quad (58)$$

In this context, let $\boldsymbol{\zeta}(k) := \boldsymbol{\Gamma}(k) - \mathbf{Q} - \boldsymbol{\Phi}(k)^T \mathbf{R}\, \boldsymbol{\Phi}(k)$ and $\hat{\boldsymbol{\xi}}(k+1) = \mathbf{A}(s(k+1)) + \mathbf{B}(s(k+1))\boldsymbol{\Phi}(k)$. Since Eq. (48) is satisfied at step k, the inequality presented in Eq. (58) holds, ensuring the feasibility of the optimization problem in Eq. (46). Considering (48) and (49), it is guaranteed that there exists $\varepsilon > 0$ that satisfies $\delta(k)\mathbf{I} - \varepsilon\boldsymbol{\Phi}(k) > 0$ for any $t > k$. Now, the stability constraint (23) guarantees that $\hat{\mathbf{x}}_p(k|k) := \hat{\mathbf{x}}(k)$, $\mathbf{u}(k|k)$, and $\hat{\mathbf{x}}_p(k+1|k)$ converge to zero, since $\mathbf{Q}\ \&\ \mathbf{R} > 0$, and $\boldsymbol{\Gamma}(k) > \varepsilon\,\mathbf{I}$. In addition, it is concluded from section 2.2 that the estimated state $\hat{\mathbf{x}}(k)$ will converge to the system state $\mathbf{x}(k)$ as $k \to \infty$. Therefore, the feasibility of solving the optimization problem (46) guarantees the asymptotic robust stability, (i.e., $\mathbf{x}(k) \to 0$ as $k \to \infty$). Then, the proposed robust output feedback MPC scheme is described as $\min_{\mathbf{u}(k|k),\, \mathbf{Y}(k),\, \boldsymbol{\Phi}(k),\, \mathbf{X}(k)} \delta(k)$ subject to (12), (13), (47)–(51) and at each step k, to implement the first control input $\Delta u(k|k)$ and $u(k|k)$, the optimal control sequence $u(k+i|k)$ will be determined by solving the aforementioned optimization, considering the measured output $y(k)$ and the time-varying parameter $s(k)$.

It is worth mentioning that the linear matrix inequalities (LMIs) derived in this paper were implemented and solved in MATLAB using the YALMIP toolbox interfaced with the MOSEK solver. To ensure reliable numerical conditioning, all weighting matrices were appropriately scaled, and a small regularization term $\varepsilon = 10^{-6}$ was added where necessary. The condition numbers of the resulting LMIs were monitored throughout the simulations and remained below 10^6, indicating well-posed and numerically stable problems. No solver failures or numerical instabilities were observed in any of the tested cases, including both predefined and random switching scenarios.

ACCEPTED MANUSCRIPT

2.4 Comparative Analysis with Existing Quasi-min–max Approaches

To clarify the specific contributions of the proposed cost function relative to prior quasi-min–max MPC formulations, Table ١ summarizes the key structural differences with Lu and Arkun [23]and Park et al [٢٩].

Table ١ Structural comparison of the proposed approach with Lu and Arkun [٢٣] and Park et al. [29]

Proposed approach	**Park et al. [29]**	**Lu & Arkun [23]**	**Feature**
Output feedback	Output feedback	State feedback	Feedback type
$\Delta u(k)$ (rate of change)	Absolute u(k)	Absolute u(k)	Cost function penalty
Explicit separation of deterministic term $B_k.u(k-1)$ from uncertain propagation	$\hat{z}((k+1\|k)) = \hat{x}(k+1)$, no further decomposition	—	Predictive dynamics
Zero by construction ($u(-1)=0$ convention + Δu - based cost)	Not enforced	Not enforced	Initial control value
Directly penalized via $\Delta u(k)$ term	Not addressed	Not addressed	Switching-induced fluctuation mitigation

3. SIMULATION RESULTS

To demonstrate the effectiveness of the proposed quasi-min-max approach for output feedback model predictive control in comparison with the prior research [29], a numerical example is evaluated. The linear parametric variable (LPV) system switches between three different system dynamics, which are given by:

$$\mathbf{x}(k+1) = \mathbf{A}_i\left(a(k), b(k)\right)\mathbf{x}(k) + \mathbf{B}_i\left(\gamma(k)\right)\mathbf{u}(k)$$
$$\mathbf{y}(k) = \mathbf{C}_i\mathbf{x}(k) \tag{59}$$

where,

ACCEPTED MANUSCRIPT

$$\mathbf{A}_i\left(a(k), b(k)\right)=\begin{bmatrix} 0.8500 & -0.0743\times a_i(k) \\ 0.0811\times b_i(k) & 0.9050 \end{bmatrix}$$
$$\mathbf{B}_i\left(\gamma(k)\right)=\gamma_i(k)\begin{bmatrix}0.1050\\0.0092\end{bmatrix},\ C_i=\begin{bmatrix}0.65 & -0.50\end{bmatrix}\quad i=1,2,3 \tag{60}$$

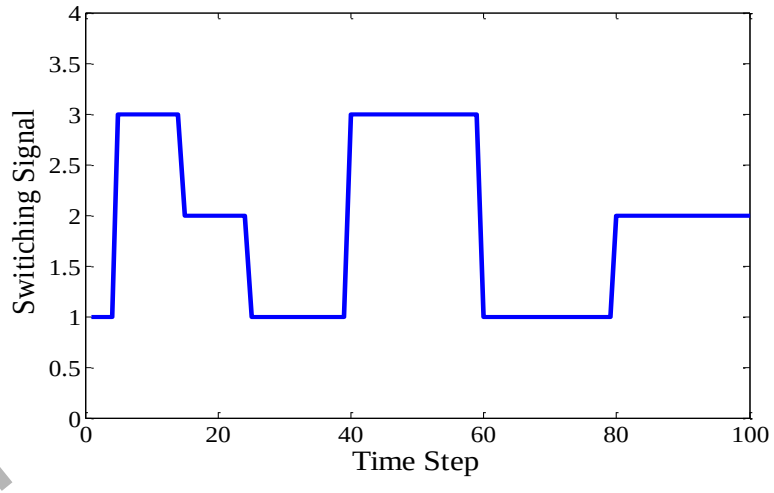
The unknown parameters are defined as $a(k)\epsilon\{1, 1.7, 2.4\}$, $b(k)\epsilon\{1, 1.5, 4.3\}$ and $\gamma(k)\epsilon\{0.33, 0.66, 1\}$, which change based on the switching signal, either dependent on or independent of the operating point of the system. The initial states of the system are selected according to Eq. (59) as $\mathbf{x}(0)=\begin{bmatrix}-1.5 & -0.2\end{bmatrix}^{\mathrm{T}}$, and the initial states of the observer are selected by Eq. (2) as $\hat{\mathbf{x}}(0)=\begin{bmatrix}0.5 & 1\end{bmatrix}^{\mathrm{T}}$. Taking into account the input constraint introduced by Park et. al.[29], $|\mathbf{u}(k)|<1;\ k\geq 0$, and the decay rate, the weighting matrix and the state observer gain are obtained as given in Table ۲.

Table ۲ Observer parameters obtained from **Theorem1**

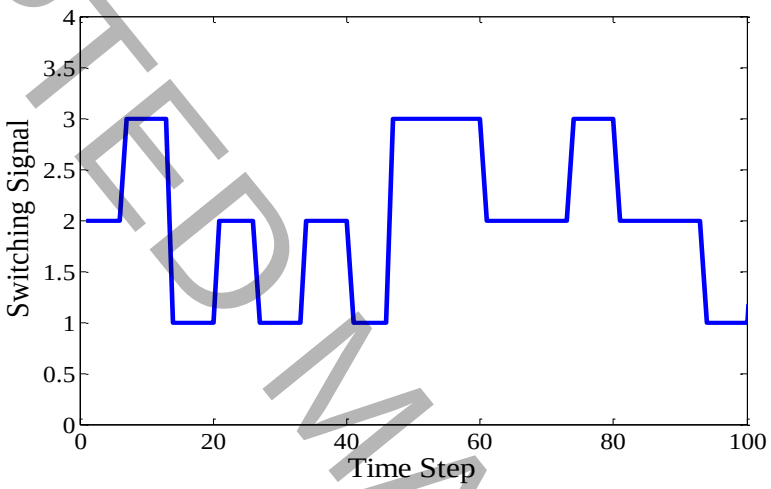
Parameters	Final value
Decay rate	$\rho=\sqrt{0.7}$
Weighting matrix	$\mathbf{L_e}=\begin{bmatrix}1 & 0\\0 & 1\end{bmatrix}$
observer gain	$\mathbf{L_o}=\begin{bmatrix}0.4631 & -1.4336\end{bmatrix}^{\mathrm{T}}$

To determine the optimal control input $\mathbf{u}(k)$, which satisfies the aforementioned input constraint, one should solve the optimization problem in Eq. (12). Considering the other design parameters as $\mathbf{L}=\begin{bmatrix}1 & 0\\0 & 1\end{bmatrix}$, $\mathbf{R}=1$ and $\epsilon=0.001$, the general problem will be solved online. In most cases, it is assumed that the changes in the system's parameters are imposed by the operating point of the system. As a general case, consider the switching signal between different piecewise linear dynamic systems independently. Hence, for generating a general condition representing the system dynamics at any specified time step, two different switching signals are used: the defined switching signal (DSWS) and the random switching signal (RSWS) (Fig. 1).

ACCEPTED MANUSCRIPT



(a)



(b)

Fig. 1 The representation of a dynamic system by the use of switching signals: (a) defined switching signal (DSWS) (b) random switching signal (RSWS)

4. RESULTS AND DISCUSSIONS

The aforementioned method was implemented on an LPV system that exhibits switching characteristics in its dynamics. Fig.2 shows a comparison of the system output for the proposed improved quasi-min-max approach with output feedback model predictive control versus the method described in the research [23, 29]. The RMS of the system output for [29] and the proposed modified approach are 0.1729 and 0.1749, respectively — a marginal increase of approximately 1.2%. This small degradation in tracking performance is an expected and interpretable consequence of the **Δu**-based cost formulation: by penalizing the rate of change in control effort rather than its absolute magnitude, the optimizer no longer directly minimizes $\mathbf{u}(k)$ at each step, trading a small amount of tracking optimality for the reduced switching-induced

ACCEPTED MANUSCRIPT

control fluctuation demonstrated in Fig. 5 This trade-off is analogous to that observed in rate-weighted DMC/MPC schemes in industrial practice, and is consistent with the practical objective of this work — namely, smoother, implementation-ready control signals — rather than representing an unexplained degradation in performance. The RMS of the system output for the proposed improved MPC with output feedback compared to the one in [29]is presented in Fig. 3 for a given switching signal**.**

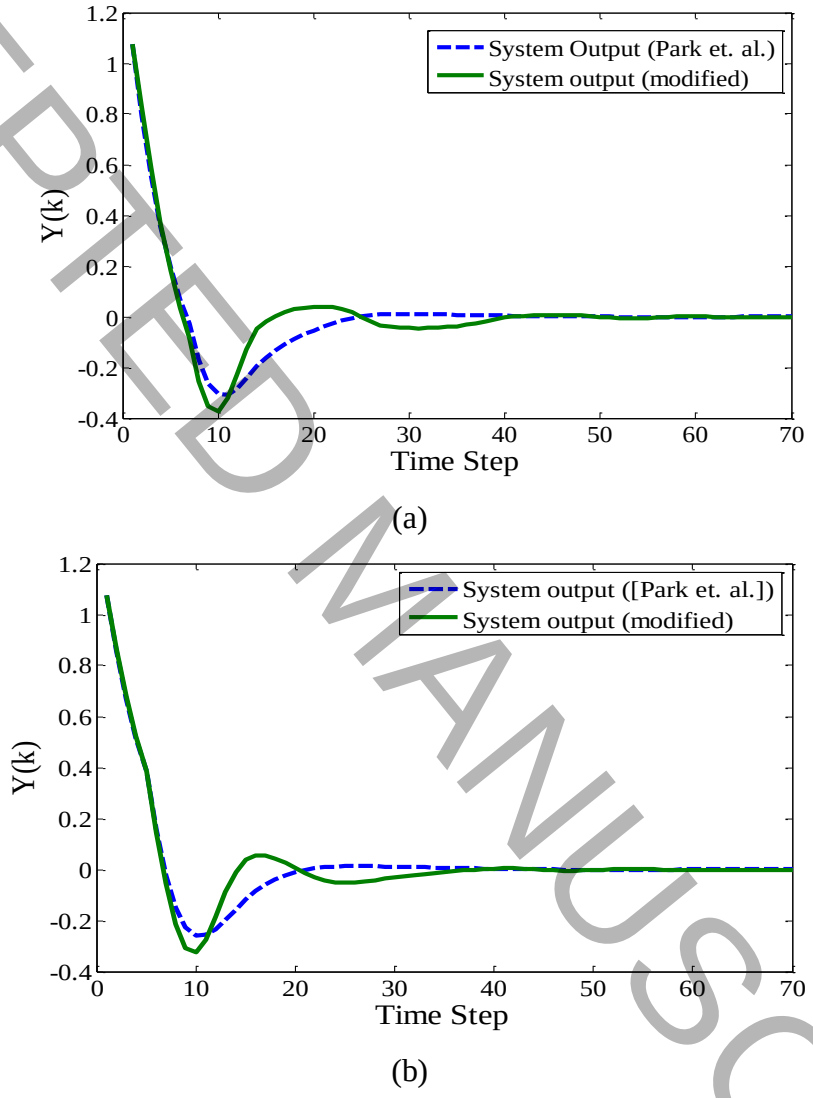


Fig. 2 System output; a comparison between the improved approach vs [29]for $\mathbf{Q}=1\times\mathbf{I}$ and $\mathbf{R}=1$, (a) DSWS (b) RSWS

The results presented in this figure show that by increasing the parameter $\mathbf{Q}$ while keeping $\mathbf{R}$ constant ($\mathbf{R}=1$), the reported RMS does not change significantly. Therefore, for designing the controller, the values for the weighting matrices $\mathbf{R}$ and $\mathbf{Q}$ are selected as $\mathbf{Q}=1\times\mathbf{I}$ and $\mathbf{R}=1$.

ACCEPTED MANUSCRIPT

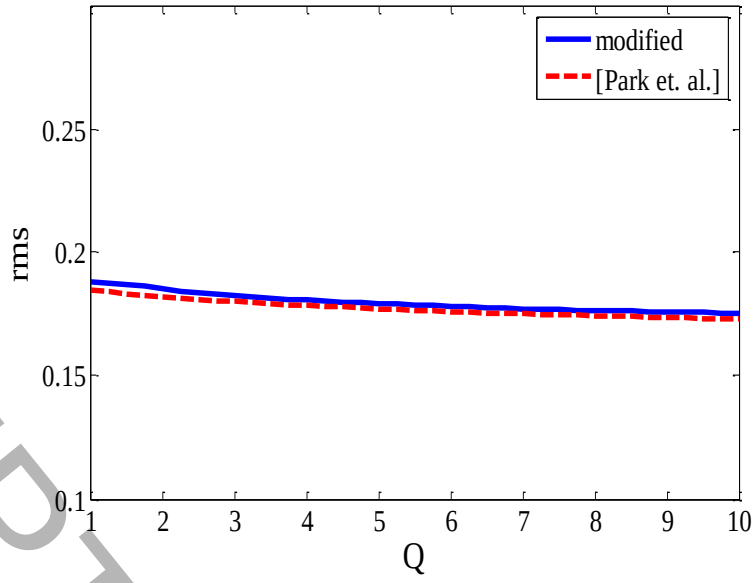
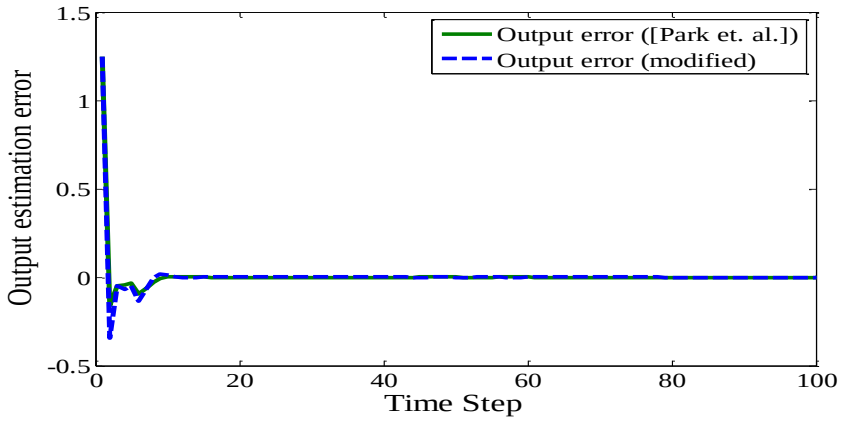


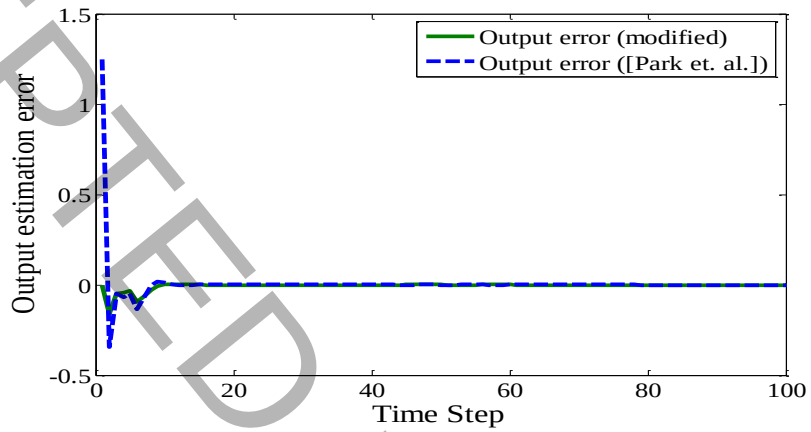
Fig. 3 The root mean square (RMS) of the system output; a comparison between the improved approach vs.[29], for the variation of $\mathbf{Q}$ and $\mathbf{R}=1$ for DSWS

As observed in the results, despite the significant changes made in the definition of the cost function to minimize or eliminate unwanted switching in the control input, both approaches exhibit similar behavior in regulating the outputs of the control system. Fig. 4 presents a comparison between the estimation errors of the system output for both approaches. Although both methods show good convergence in tracking the estimated output values, the proposed approach demonstrates faster convergence with minimal deviation even at the initial times. Fig. 4 illustrates that the proposed observer performs well in both approaches.

ACCEPTED MANUSCRIPT



(a)

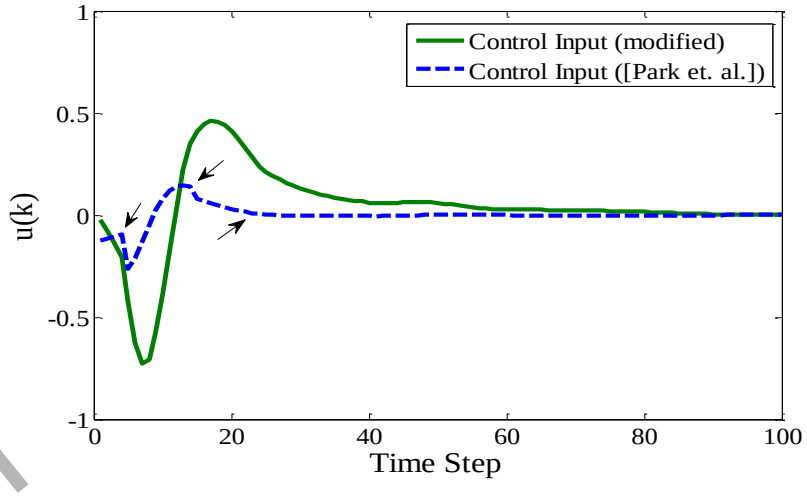


(b)

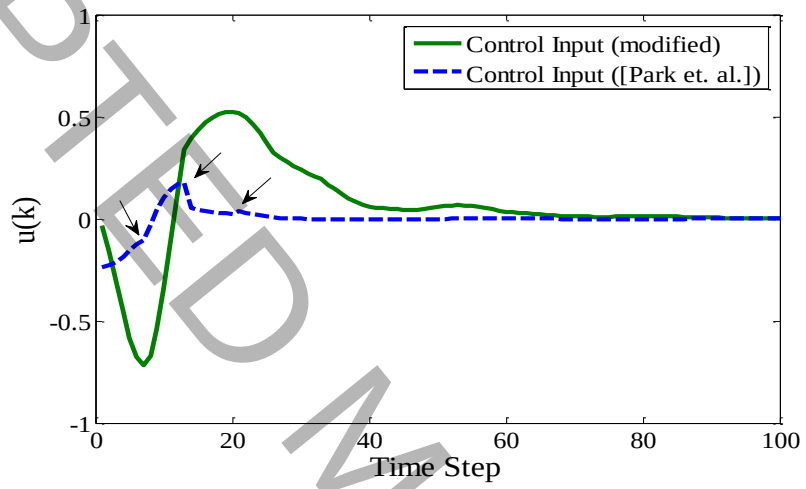
Fig. 4 Estimation error of the system output; a comparison between the improved approach vs. [29]for $\mathbf{Q}$ and $\mathbf{R}=1$, (a) DSWS (b) RSWS

Fig. 5 depicts the control input which is obtained by solving the optimization problem in Eq. (46) at each sampling instant. The arrows in Fig. 5 indicate the switching instants of the system dynamics. As shown, both the proposed approach and the method presented by Park et al. [29]satisfy the input constraint $|\mathbf{u}(k)|<1; k\geq 0$. However, the proposed approach exhibits smoother control behavior with reduced input fluctuations during switching events. Furthermore, the control input is initialized at zero, i.e., $(\mathrm{u}(0)=0)$.

ACCEPTED MANUSCRIPT



(a)



(b)

Fig. 5 The control input of the system; a comparison between the improved approach vs.[29] for $\mathbf{Q}$ and $\mathbf{R}=1$, (a) DSWS (b) RSWS. Arrows show the points when the switches occur in the dynamics of the system

It also enables to reduce system uncertainties and improves tracking behavior. However, the switching phenomenon is more pronounced when random switches occur between different linear dynamics of the system (Fig.5-b).

Fig. 6 illustrates the results of control inputs over time while varying the weighting parameters. In this scenario, the proposed modified approach in the current research demonstrates superior performance compared to [23, 29]. The explanation for this can be attributed to the cost function. The modification in this approach is due to its operation at the coordinate origin, resulting in a change in the cost function.

As shown in Fig. 6, the effectiveness of the proposed method in controlling inputs is evident. The proposed method ensures that the initial control input remains zero and minimizes sudden changes in the signal due to switches in the system dynamics. In this regard, the proposed method exhibits

ACCEPTED MANUSCRIPT

relatively better performance compared to [29]. The ratio **R/Q** governs a trade-off embedded directly in the LMI stability constraints rather than merely scaling the control signal. As **Q** increases relative to **R**, the state-penalty term $\hat{\mathbf{x}}_p^T \mathbf{Q} \hat{\mathbf{x}}_p$ in Eq. (47) dominates the cost structure, requiring a larger $\delta(k)$ to satisfy the LMI (47)–(48) for a given predicted state. Since the input-constraint LMI (44) bounds the admissible control set in terms of $\delta(k)$ and $\mathbf{\Phi}(k)$, a larger $\delta(k)$ tightens this bound, pushing the optimal **u** *(k)* closer to its saturation limit — consistent with the increased control effort observed in Fig. 6 as **Q** grows. Notably, Fig. 3 shows that this increased control effort yields little corresponding improvement in RMS output, indicating that beyond a moderate **Q**, the additional control effort primarily tightens the stability margin rather than improving tracking performance. This motivates the choice of **Q** = 1×**I** and **R = 1** adopted in this study, which keeps the RMS error low while avoiding unnecessary control effort and stability-margin tightening.

This improvement is attributed to the reduction of uncertainties' effects on system robustness achieved by the MPC approach, which modifies the control law and makes the weighting matrices independent of undefined parameters. Consequently, it becomes possible to mitigate unwanted switches and discontinuities in control efforts while guaranteeing the initial value of the control signal to be zero at $t = 0$.

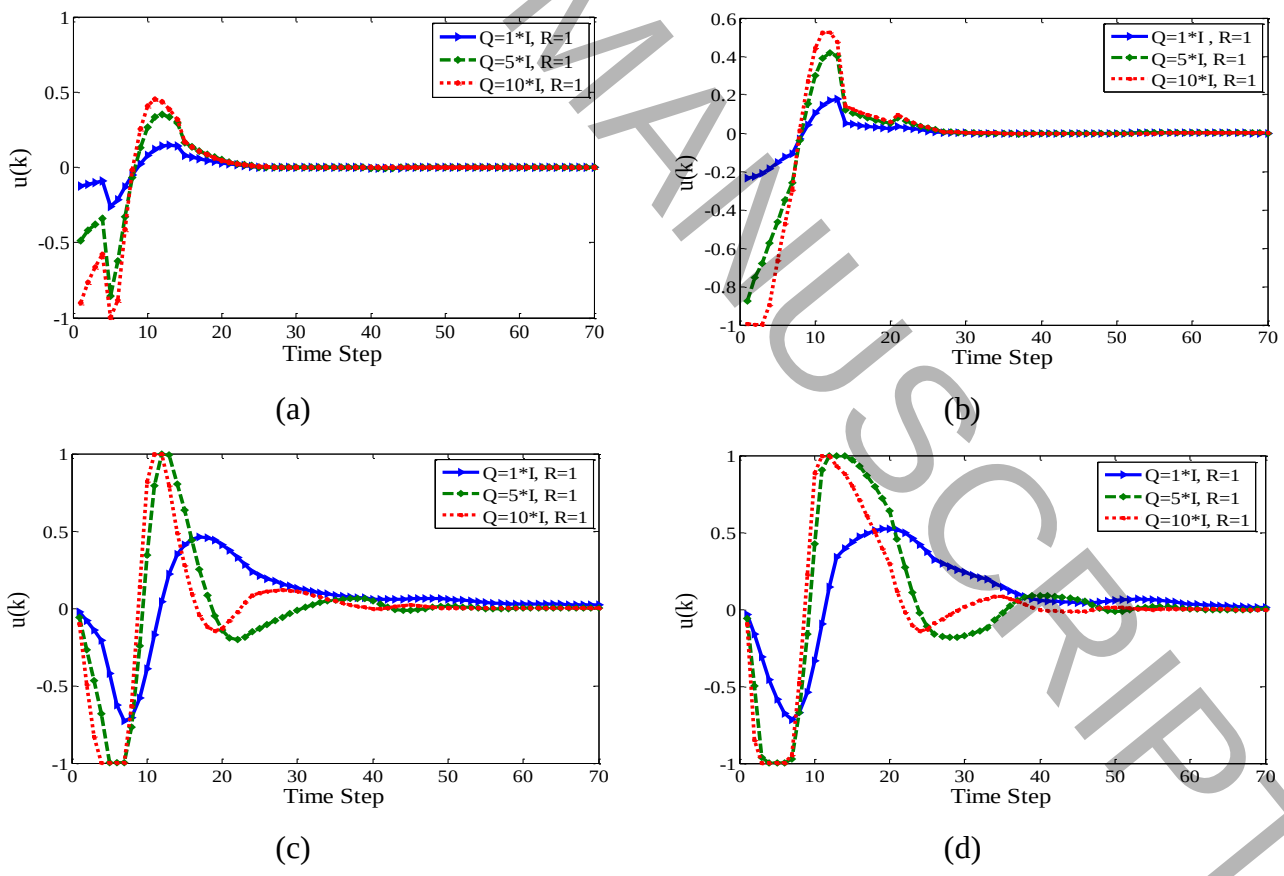


Fig. 6 Comparison of the system control input; (a) DSWS of [29],(b) RSWS of [29], (c) DSWS of the modified algorithm, (d) RSWS of modified algorithm

ACCEPTED MANUSCRIPT

In addition to the numerical benchmark presented above, the practical applicability of a closely related output-feedback MPC formulation — incorporating one-step predictive dynamics and a Δu-based cost function — has been experimentally validated on a haptic robotic training system in our related work [39]. In that study, the controller was applied to a third-order (nx=3) hybrid LPV system representing a Novint Falcon parallel robot interacting with switching tissue-fracture dynamics; the haptic device, which naturally exhibits parameter-varying and uncertain dynamics due to human-operator interaction and mechanical nonlinearities, was successfully stabilized under real sensor noise and time-varying interaction forces recorded from multiple experimental trials. These experimental results, together with the numerical example presented above, support the practical applicability of the proposed formulation beyond the second-order simulation reported here.

While the present study focuses on RMS output tracking as the primary performance indicator, a comprehensive quantitative comparison — including control energy, settling time, a quantitative index of switching-induced control variation (e.g., total variation of $\boldsymbol{u}(k)$ at switching instants), and closed-loop sensitivity to measurement noise in the switching signal $s(k)$ — is left for future work.

5. CONCLUSION

Many physical systems exhibit nonlinear dynamics that cannot be adequately represented by linear models. Although nonlinear control methods exist, they are often computationally expensive and difficult to implement. Linear parameter-varying (LPV) systems offer a practical solution by generalizing nonlinear dynamics through a collection of linear models while remaining computationally tractable. Nevertheless, mode switching in such systems can induce instability and sudden jumps in the control signal. Model predictive control methods have been widely applied to LPV systems; however, existing formulations often produce non-uniform control signals and do not guarantee a zero initial control action at the start of operation. These limitations are critical for achieving consistent performance in real-world applications such as haptic virtual reality, teleoperation, and robotic systems.

A modified robust output-feedback MPC algorithm based on the quasi-min–max method is proposed for LPV and hybrid systems. An offline robust state observer is first designed. A cost function that penalizes the input increment Δu, together with consistent one-step predictive dynamics, is then introduced. This formulation reduces unwanted disturbances caused by switching in the control

ACCEPTED MANUSCRIPT

signal, ensures convergence of the output to the desired values, and maintains robust stability under input constraints. Moreover, the initial value of the control effort is zero by construction, a property of practical importance.

The proposed algorithm is evaluated on a hybrid system under two scenarios: a predefined switching signal and a random switching signal. In both cases, closed-loop stability and observer performance are confirmed, and the control input starts from zero. In addition, the switching-induced control fluctuations observed in the baseline method [29] are substantially reduced, as illustrated in the simulation results, although they are not entirely eliminated—a trade-off that is analyzed in the comparative section of the paper. Overall, the proposed modified MPC scheme for linear parameter-varying and hybrid systems guarantees robust stability of the output-feedback closed-loop system and ensures convergence of the optimization subject to input constraints.

6. DATA AVAILIABILITY

All data generated or analysed during this study are included in this published article.

7. CONFILICT OF INTEREST

The authors declare no conflict of interests.

8. Acknowledgment

The authors would like to express their sincere gratitude to Dr. Ali Ebrahimi for his valuable insights and expertise, which greatly contributed to this research. The authors also gratefully acknowledge the Bioinspired System Design Laboratory, Department of Biomedical Engineering, Amirkabir University of Technology (Tehran Polytechnic), for its support of this research.

9. REFERENCES

[1] J. Park, T. Kim, T. Sugie, Automatica Output feedback model predictive control for LPV systems based on quasi-min–max algorithm, Automatica, 47(9) (2011) 2052–2058.
[2] S. Sadeghnejad, F. Farahmand, G. Vossoughi, H. Moradi, S. Mousa Sadr Hosseini, Phenomenological tissue fracture modeling for an Endoscopic Sinus and Skull Base Surgery training system based on experimental data, Medical Engineering and Physics, 68 (2019) 85–93.
[3] F. Khadivar, S. Sadeghnejad, H. Moradi, G. Vossoughi, F. Farahmand, Dynamic Characterization of a Parallel Haptic Device for Application as an Actuator in a Surgery Simulator, 5th RSI International Conference on Robotics and Mechatronics, IcRoM 2017, (IcRoM) (2017) 186–191.
[4] A. Morsi, H.S. Abbas, A.M. Mohamed, Wind turbine control based on a modified model predictive control scheme for linear parameter-varying systems, IET Control Theory & Applications Research, (2017) 3056–3068.
[5] A. Pavlov, I. Shames, C. Manzie, Minimax strategy in approximate model predictive control, Automatica, 111(xxxx) (2020) 108649.
[6] H. Kolbari, S. Sadeghnejad, M. Bahrami, K.E. Ali, Adaptive Control of a Robot-Assisted Tele-Surgery in Interaction With Hybrid Tissues, Journal of Dynamic Systems, Measurement and Control,

ACCEPTED MANUSCRIPT

Transactions of the ASME, 140(12) (2018).
[7] H. Kolbari, S. Sadeghnejad, M. Bahrami, A. Kamali, Bilateral adaptive control of a teleoperation system based on the hunt-crossley dynamic model, International Conference on Robotics and Mechatronics,ICRoM 2015, (2015) 651–656.
[8] H. Kolbari, S. Sadeghnejad, M. Bahrami, E.A. Kamali, Nonlinear adaptive control for teleoperation systems transitioning between soft and hard tissues, International Conference on Robotics and Mechatronics, ICROM 2015, (2015).
[9] F. Khadivar, S. Sadeghnejad, H. Moradi, G. Vossoughi, Dynamic characterization and control of a parallel haptic interaction with an admittance type virtual environment, Meccanica, 55(3) (2020) 435–452.
[10] L. Cavanini, G. Cimini, G. Ippoliti, Computationally efficient model predictive control for a class of linear parameter-varying systems, IET Control Theory Appl, (2018) 1384–1392.
[11] R. Hoffmann, B. Taetz, M. Miezal, G. Bleser, S. Leyendecker, Foundations of optimal control theory, Multibody System Dynamics, 48(1) (2020) 105–126.
[12] Cutler, Ramaker, 1980_Cutler-Ramaker_Dynamic-matrix-control_JACC1980, (1980).
[13] P. Lundström, J.H. Lee, M. Morari, S. Skogestad, Limitations of dynamic matrix control, Computers & Chemical Engineering, 19(4) (1995) 409–421.
[14] L. Magni, R. Scattolini, Stabilizing model predictive control of nonlinear continuous time systems, Annual Reviews in Control, 28(1) (2004) 1–11.
[15] R. Uddin, J. Ryu, Predictive control approaches for bilateral teleoperation, Annual Reviews in Control, 0 (2016) 1–18.
[16] Y.-G. XI, D.-W. LI, S. LIN, Model Predictive Control — Status and Challenges, Acta Automatica Sinica, 39(3) (2013) 222–236.
[17] T. Faulwasser, R. Findeisen, Nonlinear model predictive control for constrained output path following, IEEE Transactions on Automatic Control, 61(4) (2016) 1026–1039.
[18] P. Ojaghi, N. Bigdeli, M. Rahmani, An LMI approach to robust model predictive control of nonlinear systems with state-dependent uncertainties, Journal of Process Control, 47 (2016) 1–10.
[19] J. Wilson, M. Charest, R. Dubay, Non-linear model predictive control schemes with application on a 2 link vertical robot manipulator, Robotics and Computer-Integrated Manufacturing, 41 (2016) 23–30.
[20] G.C. Calafiore, S. Member, L. Fagiano, Robust Model Predictive Control via Scenario Optimization, IEEE Trans Autom Control, 58(1) (2013) 219–224.
[21] R. Yadbantung, P. Bumroongsri, Tube-based robust output feedback MPC for constrained LTV systems with applications in chemical processes, European Journal of Control, 47 (2019) 11–19.
[22] P. Sindareh Esfahani, J.K. Pieper, Robust model predictive control for switched linear systems, ISA Transactions, 89 (2019) 1–11.
[23] J. Control, L. Huofa, H.I. Marrani, A new robust LMI-based model predictive control for continuous-time uncertain nonlinear systems, Automatika, (2020) 670–681.
[24] Y. Lu, Y. Arkun, Quasi-min-max MPC algorithms for LPV systems, Automatica, 36(4) (2000) 527–540.
[25] A. Asuk, P. Trodden, Feedback-Optimizing Model Predictive Control for Constrained Linear Systems, IFAC-PapersOnLine, 54(6) (2021) 43–49.
[26] A. dos Reis de Souza, D. Efimov, T. Raissi, Robust Output Feedback MPC for LPV Systems Using Interval Observers, IEEE Transactions on Automatic Control, 67(6) (2022) 3188–3195.
[27] W. Gu, J. Yao, Z. Yao, J. Zheng, Output feedback model predictive control of hydraulic systems with disturbances compensation, ISA Transactions, 88 (2019) 216–224.
[28] Z. Wan, M. V Kothare, Robust output feedback model predictive control using off-line linear matrix inequalities, Journal of Process Control, 12 (2002) 763–774.
[29] M. Moraris, Robust Constrained Model Predictive Control using Linear Matrix Inequalities *, Automatica, 32 (1996) 1361–1379.
[30] I. Nodozi, M. Rahmani, LMI-based model predictive control for switched nonlinear systems, Journal of Process Control, 59 (2017) 49–58.

ACCEPTED MANUSCRIPT

[31] F. ed Zhang, THE SCHUR COMPLEMENT AND ITS APPLICATIONS, Springer Science & Business Media., 4 (2006).
[32] Hossam Seddik Abbas, Linear parameter-varying model predictive control for nonlinear systems using general polytopic tubes, Automatica, 160 (2024).
[33] M. Bujarbaruah, U. Rosolia, Y.R. Stürz, X. Zhang, F. Borrelli, Robust MPC for LPV systems via a novel optimization-based constraint tightening, Automatica, 143 (2022).
[34] X. Bin Ping, P. Wang, J.F. Zhang, A Multi-step Output Feedback Robust MPC Approach for LPV Systems with Bounded Parameter Changes and Disturbance, International Journal of Control, Automation and Systems, 16(5) (2018) 2157–2168.
[35] C. Verlioek, H.S. Abbas, R. Totli, S. Haesaert, Data-Driven Predictive Control for Linear Parameter-Varying Systems, IFAC-PapersOnLine, (2021) 101–108.
[36] Y. Xie, J. Berberich, F. Brändle, F. Allgöwer, Data-Driven Min-Max MPC for LPV Systems with Unknown Scheduling Signal, (2024).
[37] L. Carvalho, M.V.S. Costa, L.H. Macedo, E. V. Fortes, A novel approach for robust model predictive control applied to switched linear systems through state and output feedback, Journal of the Franklin Institute, 360(2) (2023) 1184–1206.
[38] C. Hu, Z. Wu, Model predictive control of switched nonlinear systems using online machine learning, Chemical Engineering Research and Design, 209 (2024) 221–236.
[39] S. Sadeghnejad, F. Khadivar, M. Esfandiari, G. Amirkhani, H. Moradi, F. Farahmand, et al., Using an Improved Output Feedback MPC Approach for Developing a Haptic Virtual Training System, Journal of Optimization Theory and Applications, 198(2) (2023) 745–766.

ACCEPTED MANUSCRIPT